Post-print of: Narożny M., Żakowski K., Darowicki K.: Time evolution of Electrochemical Impedance spectra of cathodically protected steel in artificial seawater. CONSTRUCTION AND BUILDING MATERIALS. Vol. 154, (2017), s. 88-94. DOI: 10.1016/j.conbuildmat.2017.07.191

Time evolution of Electrochemical Impedance spectra of cathodically protected steel in artificial seawater

M. Narozny, K. Zakowski, K. Darowicki

Department of Electrochemistry, Corrosion and Materials Engineering, Chemical Faculty, Gdansk University of Technology, 11/12 Narutowicza St., 80-233 Gdansk, Poland

highlights

- Usability of EIS data for better cathodic protection control was investigated.
- Time evolution of Electrochemical Impedance spectra was evaluated.
- Quantity of physical and electrochemical processes was evaluated by usage of Chi2 function. •

EIS proved to be useful for hydrogen evolution detection.

abstract

Usability of Electrochemical Impedance Spectroscopy data for better cathodic protection control was investigated. Carbon steel – S235JR2 grade specimen were exposed in artificial seawater environment. Samples were polarized and their potentials corresponded to four different cathodic protection degrees. Time evolution of Electrochemical Impedance spectra was investigated. Goodness of fit function (X^2) was analysed in terms of proper time-constant quantity determination. It was possible to observe and detect occurrence of new phenomena by X^2 evaluation. Weight-loss corrosion coupons were used to calculate corrosion rates. At initial stage of exposition impedance measurements complemented proper protection potential data. Quantity of physical and electrochemical processes was evaluated and linked to the state of specimen providing valuable supplementary data. EIS proved to be useful for hydrogen evolution detection which is a great risk which has to be recognised and prevented.

Keywords: Cathodic Protection, Seawater, Electrochemical Impedance Spectroscopy, Steel

1. Introduction

Organic coatings combined with cathodic protection (CP) are currently the most widely utilised means of corrosion protection for buried and immersed steel structures [1]. These corrosion protection technologies are complementary. Organic coatings form a physical barrier to isolate a construction from environment [2–4]. However, to achieve a full degree of long lasting corrosion protection a proper cathodic protection (CP) system has to be implemented as well. Cathodic calcareous sediments which may form on a CP protected surface also provide a coating-like effects. Oxygen diffusion to the protected surface is slowed down and effective electrode surface area is decreased. Thus sediments reduce protection current demand as well. Typical cathodic sediments mostly consist of $CaCO_3$ and $Mg(OH)_2$ [5].

Protection current can be either supplied by sacrificial anodes or by an Impressed Current Cathodic Protection (ICCP) [6,7]. Sacrificial anodes are passive and do not require any additional equipment. However there are also methods for driving galvanic anodes [8,9]. Cathodic rectifiers (ICCP) are far more complex devices [10]. They are either manually or microcomputer controlled units. Thus CP rectifiers provide better control of cathodic polarization conditions than galvanic anodes. Microcomputer (uC) driven CP rectifiers might have additional features, such as an internal GPS module, synchronous on/off potential switch, data logger and data transmission device i.e. GSM, intranet, landline [11,12] enabling access to accurate and real time information. Furthermore, application of an uC gives an opportunity to introduce additional functionality to the CP rectifier, such as electrical resistance corrosion probes inspection or EIS probes [13,14].

Knowledge of surface condition is crucial to efficient corrosion protection. Electrochemical Impedance Spectroscopy (EIS) is a technique capable of providing valuable electrical data which can be associated with surface evolution and kinetics of electrochemi-

http://dx.doi.org/10.1016/j.conbuildmat.2017.07.191

cal processes. Application of this technology as a diagnostic tool for CP systems has been proposed. Proper data interpretation of collected EIS data could reduce costs of CP maintenance, especially when visual examination costs are considered. There are several controversies regarding cathodic protection criteria, especially with determination of instantaneous corrosion rates in cathodic protection conditions. Furthermore potential criteria and widely used potential measurements give no information about corrosion rates. Thus the ultimate goal is knowledge of momentary corrosion rates of a cathodically polarized sample.

In this paper an experiment involving EIS investigation of steel samples polarized to different cathodic protection levels has been proposed. Time evolution of EIS spectra and determined corrosion rates have been investigated. Every EIS data set was fit to three cell models consisting of one, two and three time constants. Goodness of fit function (X^2) was analysed in terms of proper time-constant quantity determination, which translates to number of currently occurring phenomena and system complexity. Chi squared is a measure describing discrepancies between measured values and a model under investigation. The lower X^2 value is the better the fit is (1).

$$X^2 = \sum \frac{(measured - expected)^2}{expected} \quad (1)$$

2. Materials and methods

A set of circular S235JR2 steel samples has been prepared. Steel composition is presented in Table 1. Specimen radius equalled 6 cm and their surface area 28.25 cm^2. For preliminary EIS experiments additional round electrodes were prepared in the same manner but their area equalled 1 cm^2. Electrodes were mounted in epoxy resin and their surface was sandblasted to Sa3 NACE "white metal blast cleaning" [15].

Specimen were immersed in 30 l of artificial seawater in 50 × 20 × 30 cm tanks. The water was composed in agreement with ASTM D1141-98 standard and is presented in Table 2 [16]. Salts with lower content than KBr were not used in the experiment.

For long exposures four potentials corresponding to different cathodic protection levels were chosen (Table 3). Mesh mixed metal oxide auxiliary electrodes (15 × 20 cm) and saturated $Zn|ZnSO_4$ reference electrodes were used. The auxiliary electrode – anode were placed approximately 40 cm away from the working electrodes to ensure uniform current distribution. Reference electrode was placed close to the specimen to diminish IR related potential drop. For every CP protection level a dedicated potentiostat was used.

Samples were exposed to artificial seawater for approximately 9 months. Throughout the entire course of the experiment EIS Electrochemical Impedance Spectroscopy measurements were performed. Prior to the long term exposure also preliminary EIS tests were carried out on smaller (1 cm^2) electrodes. For both exposures same sample surface preparation method and EIS experiment conditions were chosen. Preliminary EIS experiments were conducted in order to investigate if there are any features in EIS spectra which could be linked to corrosion rates and potential cathodic protection criteria at various cathodic potentials.

Amplitude of the perturbation signal equalled 15 mV and frequencies ranged from 0.05 to 50 kHz. In the initiatory experiment the DC offset ranged from 0 mV to −450 mV against Open Circuit Potential (OCP), EIS spectra were measured every −25 mV. The OCP of the specimen corresponds to approximately −695 mV against Ag|AgCl|Seawater reference electrode.

During the long term exposure EIS experiments were performed at DC offset potentials corresponding to the chosen cathodic protection levels (Table 3). Gamry Interface 1000 potentiostat was used to drive the experiments.

In order to identify more rapid changes in the specimen at the beginning of the exposures, shorter time intervals between measurements were selected. They equalled from 2 to 7 days. As the exposures proceed the intervals were increased to approximately 30 days.

In order to determine corrosion rate of the samples weight loss coupons were manufactured. Coupons' surface was also sandblasted to the Sa3 – NACE "white metal blast cleaning" in order to achieve exactly the same degree of surface preparation as the electrodes [15].

3. Results and discussion

EIS spectra obtained during the preliminary experiment are presented in Figs. 1 and 2. Several states of the system can be distinguished from EIS spectra, their correspondence to different cathodic protection levels and electrode potentials. When a specimen was cathodically polarized the low-frequency impedance of the system increased. This occurred until potential of approximately −0.125 V vs OCP was reached (Fig. 1). The low frequency phase angle shifted towards lower frequencies indicating reduced reaction time constant. Between −0.125 V and −0.375 V it was hard to distinguish local phase angle minimum due to its flattening. Below −0.375 V vs OCP low frequency resistance decreased because of water decomposition and hydrogen evolution reaction. Equivalent R(Q(R(QR))) circuit model was proposed with two time constants. Electrolyte resistance and charge transfer resistance in function of potential are presented in Figs. 3 and 4 respectively. Calculated electrolyte resistance was potential independent and equalled approximately 5 Ω. Initial low charge transfer resistance could be explained by occurrence of two reactions – iron oxidation and hydrogen reduction. Charge transfer resistance reached its maximum of ∼13,5 kΩ at −175 mV vs OCP (−870 mV vs Ag|AgCl| Seawater electrode) due to diffusion limitation of oxygen transport. When potential equalled −870 mV vs Ag|AgCl|Seawater DNV RP-B401 cathodic protection criterion for aerobic conditions was met [17]. At lower potentials charge transfer resistance dropped down due to oxides and hydroxides species reduction and ultimately water decomposition [18–20]. Goodness of fit was satisfactory and equalled less than 10^{-4}. This indicates that techniques such as EIS or DEIS (Dynamic Electrochemical Impedance Spectroscopy) with a probe electrode could be applied in real life situation. Complementary data to current/potential relationship could be beneficial for instance when hydrogen embrittlement risk is concerned.

Long term exposures of coated specimen were performed in order to investigate applicability of EIS to investigate changes of corrosion protected systems – coated and cathodically protected.

Exemplary EIS Nyquist and Bode plots for four protection levels are presented in Figs. 5–8. Firstly, it was noticed that spectra between analysed cathodic protection levels differ. The initial spectra were similar for all protection levels and consisted of one time constant. However they evolved in time – new time constants appeared due to surface alterations. The longer the exposure lasted the more complex the system was to analyse. Determination of a proper electrical equivalent model became formidable. Determining numerical relations linked to corrosion rate was even harder. Only a few representative spectra are presented in the graphs to make the data more accessible to the viewer. All of the plots illustrated below develop gradually.

A free-corroding sample can be considered as a reference. According to the impedance spectra the electrolyte resistance was consistent and equalled approximately 1–2 Ω. The low frequency impedance limit of the sample altered with time, ranging from 20 to 150 Ω. Initially the impedance modulus increased but over time it started to decline. The initial increase of sample's

Table 1
Composition and ultimate tensile strength of S235JR2 steel.

Element ultimate tensile strength	C [%]	Mn [%]	Si [%]	P [%]	S [%]	N [%]	UTS [N/mm2]
S235JR steel	0,17–0,20	Max 1,3	–	0,045	0,045	0,009	360–490

Table 2
Artificial seawater composition prepared in agreement with ASTM D1141-98.

Salt	NaCl	$MgCl_2$	Na_2SO_4	$CaCl_2$	KCl	$NaHCO_3$	KBr
Concentration [g/dm^3]	24.53	5.20	4.09	1.16	0.695	0.201	0.101

Table 3
Cathodic protection levels of the specimen chosen for the long term exposure.

Cathodic protection level	Potential vs $Zn/ZnSO_4$ (saturated) electrode	Potential vs Ag/AgCl electrode
No protection	Free corrosion potential	Free corrosion potential
Under-protection	+288 mV	−750 mV
Complete-protection	+88 mV	−950 mV
Over-protection	−162 mV	−1200 mV

low frequency impedance could be attributed to corrosion products evolution. As the corrosion proceeded products fell apart and gradually rebuilt. This repeatable process led to surface expansion. As the exposition proceeded a second time constant appeared. The low angle phase shift at 10^4 Hz became visible, probably due to surface species evolution (see Fig. 9).

Initially only one time constant was noticeable for the under-protected sample. Features observed at high frequencies correspond to the inductive character of the apparatus and should be neglected. It is proved by the positive value of the phase angle shift. High frequency impedance limit rose in time from approximately 0,5–2 Ω. Same observations applied to the fully cathodically protected sample. The main difference between the presented spectra is the time at which a high frequency phase shift appears. For a fully protected sample it became visible after 14 days and proved to be even more pronounced after 64 days. Similarly, this feature emerged for the under-protected specimen after 130 days. During the exposure impedance modulus vs frequency logarithm evolved toward a flatter line. Nyquist spectra became flatter, more elongated. It indicated that there were several time-constants overlapping. In order to fit at equivalent circuit to the elongated Nyquist

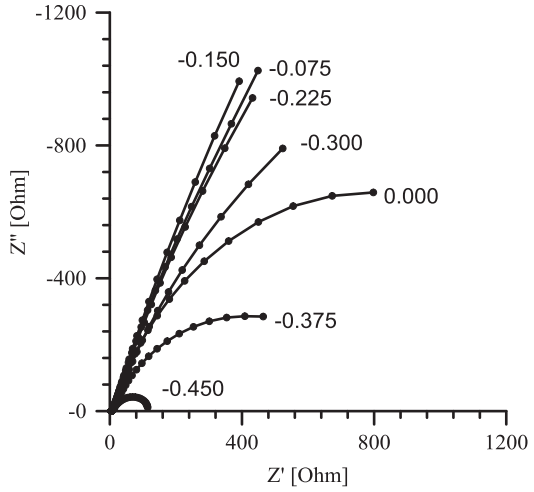

Fig. 2. Nyquist plots for 1 cm^2 S235JR2 steel samples EIS spectrograms obtained at every −25 mV from 0 to −450 mV vs OCP (−695 mV to −1145 mV vs Ag|AgCl|Seawater). Not every obtained plot is included to simplify the chart. Numbers in the plot represent potentials in [mV] at which spectra have been measured.

plot three capacitive elements had to be used. Goodness of fit was in range from 10^{-6} to 10^{-3}. Nyquist plot flattening process proceeded quicker for the fully protected sample. Due to higher degree of polarization and possible greater OH^- concentration surface evolution was faster. Ultimately spectra obtained for under-protected samples resembled those of fully protected samples but shifted in time. The low frequency impedance limit became greater in time, as presented in the Bode plots. Semicircles presented at Nyquist plots do not cross the Z' axis. It indicates that

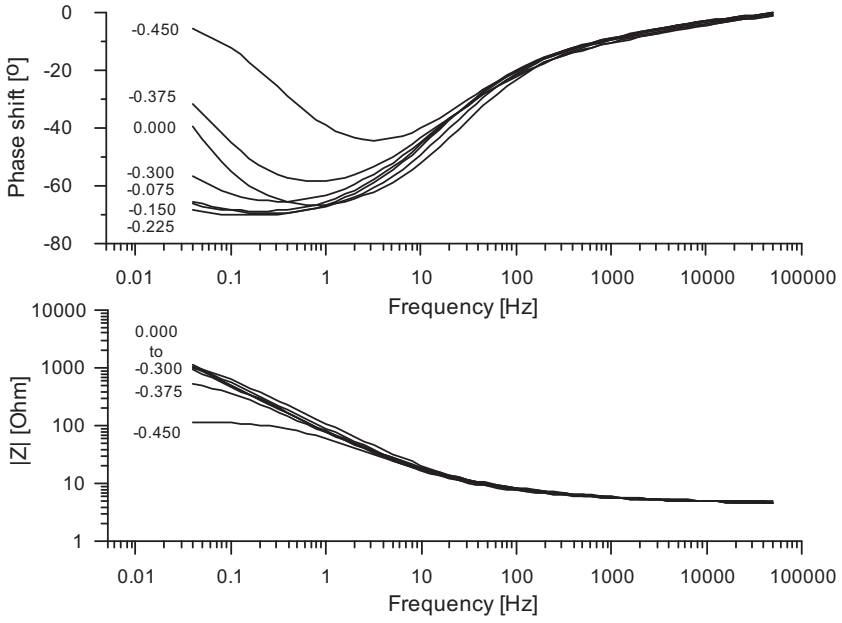

Fig. 1. Bode plots for 1 cm^2 S235JR2 steel samples EIS spectrograms obtained at every −25 mV from 0 to −450 mV vs OCP (−695 mV to −1145 mV vs Ag|AgCl|Seawater). To clarify the chart not every obtained plot is presented. Numbers in the plot represent potentials in [mV] at which spectra have been measured.

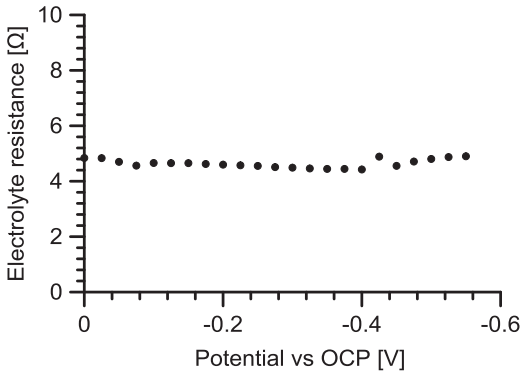

Fig. 3. Electrolyte resistance plot in a function of potential.

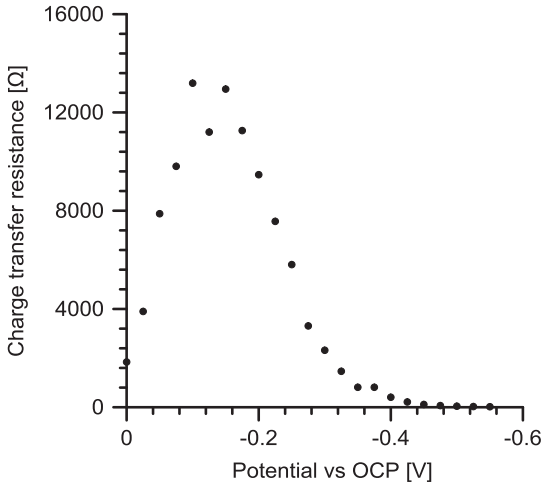

Fig. 4. Charge transfer resistance plot in a function of potential.

very slow activation processes started to govern the reaction rate. A straight Warburg line in Nyquist plot was not observed. Although spectra varied for different cathodic protection levels it was troublesome to link a parameter to a specific cathodic protection level. Initially in lower frequency range the impedance moduli for non-protected, under-protected and fully protected samples were comparable. They equalled approximately 40, 100 and 100 Ω respectively. During the entire exposure the low frequency impedance modulus limit was similar for those samples. However the low frequency impedance limit of the overprotected sample exhibited a plateau which was lower by two orders of magnitude. Thus, lower impedance limits and appearance of low frequency plateau in Bode spectrum (Nyquist spectra form full semicircles) suggested overprotection.

Finding a proper model or models for the obtained data was problematic. Instead of comparing fitted parameters an evaluation of goodness of fit was proposed. It was proved that the surface of a cathodically polarized specimen evolve and their characteristics were not the same during the entire exposure. Under-protected sample was suggested as an example. Equivalent models with one, two and three time constants were assessed. Three models were used to fit EIS experimental data: R(CR), R(C(R(CR))) and R(C(R(C(R(CR))))) respectively. Initially a single time constant model provided a satisfying degree of fit. After 100 days a rapid increase of goodness of fit factor was noticed. It indicated that the model was no longer valid and a new one with more time constants had to be introduced. Increased number of time constants suggested that new features controlling the current flow have appeared. The best model fit would be achieved with an infinite amount of time-constant elements but physical meaning of the model would be lost. Introduction of third time constant did not significantly improve goodness of fit. It indicated that there were two major processes governing the current flow.

The simplest scenario was represented by the overprotected sample. During the entire exposure there was just one time constant observed. Water composition (Table 2) and water pH (initial pH value of 8 in the bulk was measured) were favourable for calcareous layer formation. $CaCO_3$ precipitation occurs if pH is greater than 7,5. Furthermore reduction of oxygen at the cathode yields OH^- ions increasing local pH values of the electrolyte. This was proved by visual observation of layer evolution. The calcareous layer which covered the specimen after the exposure is presented in Fig. 10. High frequency impedance limit increased with time due to the growth of cathodic sediments. Initially it equalled approximately 4 Ω whereas by the end of the exposure it reached a value of 22 Ω (Fig. 8). Due to cathodic sediments growth and reduction of electrode's working surface area the Nyquist half-circles increased their radius. Thus, low frequency impedance limit increased. Water decomposition reaction slowed down due to the reduced working surface of the electrode. There were no diffusive features observed – the calcareous layer must have been porous and enabled easy mass transport of both substrates and reaction products.

Average corrosion rates determined by weight-loss corrosion coupons are presented in Table 4. Samples were marked and their weight was measured prior exposure. After exposure coupons were etched in 10% HCl acid solution with addition of 10 g/dm3 hexamethylenetetramine $(CH_2)_6N_4$ corrosion inhibitor. Under-protected sample corroded 10 times slower than the free corroding

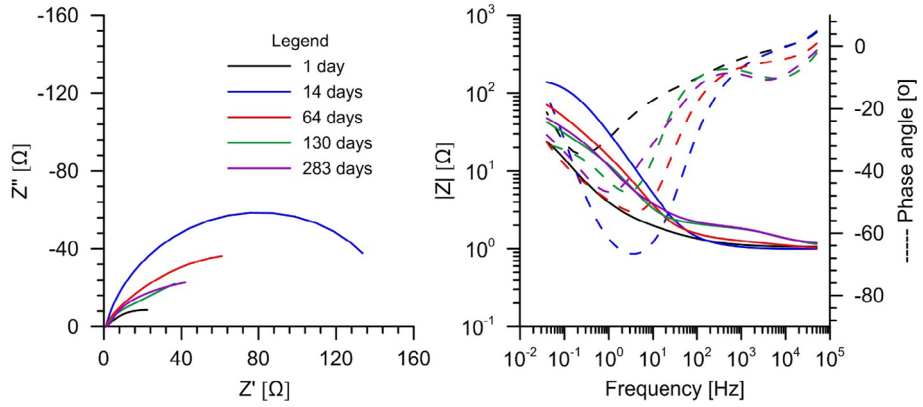

Fig. 5. Exemplary EIS Nyqist and Bode plots in time of unprotected specimen. To simplify the graph not every obtained plot is included.

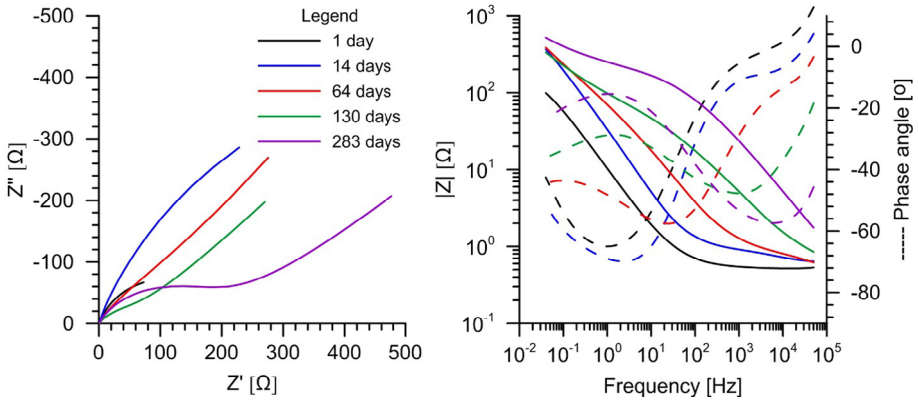

Fig. 6. Exemplary EIS Nyqist and Bode plots in time of under-protected specimen (−750 mV vs Ag|AgCl|Seawater). To simplify the graph not every obtained plot is included.

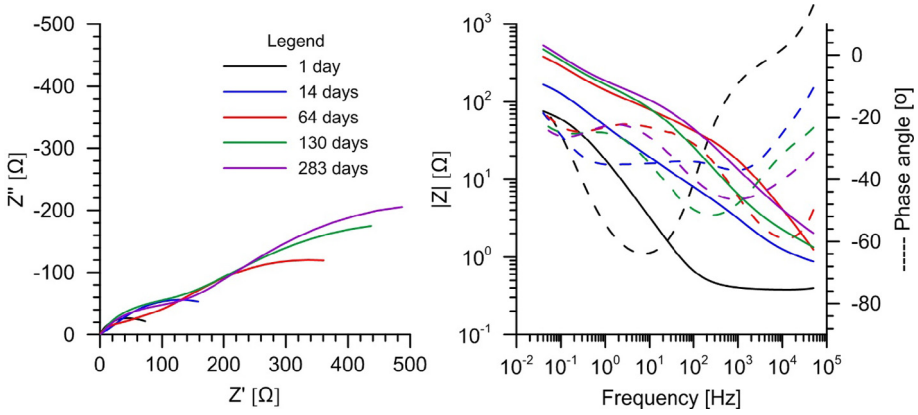

Fig. 7. Exemplary EIS Nyqist and Bode plots in time of completely protected specimen (−950 mV vs Ag|AgCl|Seawater). To simplify the graph not every obtained plot is included.

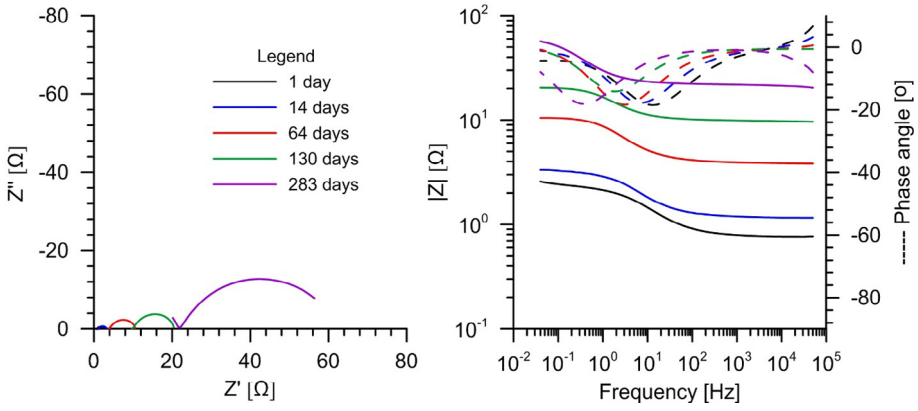

Fig. 8. Exemplary EIS Nyqist and Bode plots in time of overprotected specimen (−1200 mV vs Ag|AgCl|Seawater). To simplify the graph not every obtained plot is included.

one. Difference between over-protected and fully-protected sample is negligible. All samples except for free corroding one had their corrosion rates lower than 0,01 mm/year and met EN 12954 cathodic protection criterion [21]. The potential criterion for the under-protected sample was not met during the exposure. However the corrosion rate based criterion was satisfied, which was unintended! This proves the thesis that potential and corrosion rate based criteria are inconsistent.

4. Conclusions

Conducted experiments proved that EIS was capable of providing additional information to the cathodic protection personnel. However obtained data is often too complex for instant analysis and in-situ CP system adjustments.

For optimisation of initial cathodic protection conditions EIS yielded reasonable results and S235JR2 steel protection potential of −870 mV vs Ag|AgCl|Seawater was determined. This result is

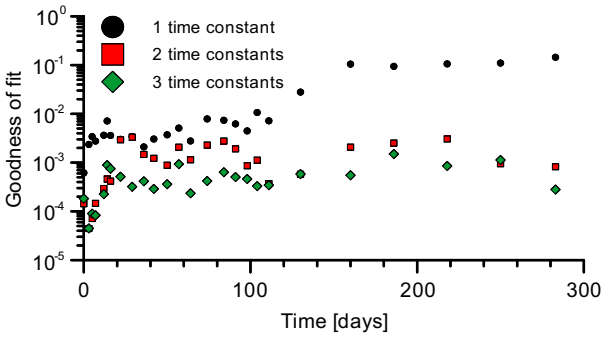

Fig. 9. Goodness of fit (X^2) of equivalent circuits consisting of one, two and three time constants. Cathodically under-protected sample.

Fig. 10. Specimen covered in calcareous cathodic products after 9 months of exposure.

in agreement with literature and requirements of international standards [14].

It can be stated that if an impedance modulus plateau at low frequency range in Bode plot is observed the sample might be overprotected. If the impedance modulus is a straight line at low frequencies the specimen might be fully protected, under protected or even not protected at all.

Although all of the occurring chemical and physical processes have similar time constants it is possible to determine their number and time of appearance by evaluation of goodness of fit function. For partially and fully-protected samples semi-circles on Nyquist plots overlap. Exact determination of occurring processes would be far-fetched. Yet Electrochemical Impedance spectroscopy techniques prove to be useful when hydrogen evolution is a risk to be recognised and prevented.

Table 4
Corrosion rates determined with weight-loss corrosion coupons.

Cathodic protection level	Corrosion rate [mm/year]
No protection	0,073
Under-protection	0,007
Complete-protection	0,003
Over-protection	0,002

Modern ICCP systems are controlled by microcomputers and additional functionality such as limited bandwidth EIS and electrical resistance corrosion probing could be easily implemented. Costs of probes fabrication and installation at new CP protected constructions could be outweighed by an additional available data. GSM data transfer availability and reduced costs open new possibilities. Thus online measurements and maintenance would even further reduce operating and labour costs of CP system.

Although the data presented in this paper is strictly based on lab results, preliminary field tests were also performed. In order to obtain proper data to analyse corrosion probes have to be used. Probes should be connected to the construction and be in proximity to reference electrode or have their own one. Other factors, for instance biocorrosion might yield even more complex results. EIS is a sufficient, widely used tool for such evaluations [22–23].

Acknowledgements

This work was supported by the National Science Centre Poland under Grant 2012/05/N/ST8/02899.

References

[1] G. Grundmeier, W. Schmidt, M. Stratmann, Corrosion protection by organic coatings: electrochemical mechanism and novel methods of investigation, Electrochim. Acta 45 (2000) 2515–2533.
[2] W. Funke, The role of adhesion in corrosion protection by organic coatings, J. Oil Colour Chem. Assoc. 68 (1985) 229–232.
[3] J. Parks, H. Leidheiser, Ionic migration through organic coatings and its consequences to corrosion, Ind. Eng. Chem. Prod. Res. Dev. 25 (1986) 1–6.
[4] M. Stratmann, R. Feser, A. Leng, Corrosion protection by organic films, Electrochim. Acta 39 (1994) 1207–1214.
[5] K. Zakowski, M. Narozny, M. Szocinski, Study of the formation of calcareous deposits on cathodically protected steel in Baltic sea water, Anti-Corros. Methods Mater. 60 (2013) 95–99.
[6] R.A. Armas, C.A. Gervasi, A. Di Sarli, S.G. Real, J.R. Vilche, Zinc-rich paints on steels in artificial seawater by Electrochemical Impedance Spectroscopy, Corr. Sci. 48 (1992) 379–383.
[7] S. Szabo, I. Bakos, Cathodic protection with sacrificial anodes, Corros. Rev. 24 (2006) 231–280.
[8] M. Narozny, K. Zakowski, K. Darowicki, Method of sacrificial anode transistor-driving in cathodic protection system, Corros. Sci. 88 (2014) 275–279.
[9] M. Narozny, K. Zakowski, K. Darowicki, Method of sacrificial anode dual transistor-driving in stray current field, Corros. Sci. 98 (2015) 605–609.
[10] S. Szabo, I. Bakos, Impressed current cathodic protection, Corros. Rev. 24 (2006) 39–62.
[11] Yajun Liu, Xianming Shi, Cathodic protection technologies for reinforced concrete: introduction and recent developments, Rev. Chem. Eng. 25 (2011) 339–388.
[12] J.P. LaFontaine, J.N. Britton, G.T. Gibson, Recent Advances in Offshore Cathodic Protection Monitoring, Corrosion 2000 Conference materials.
[13] T.J. Barlo, Cathodic protection parameters measured on corrosion coupons and pipes buried in the field, Corrosion 1998 Conference materials.
[14] M. McKenzie, P.R. Vassie, Use of weight loss coupons and electrical resistance probes in atmospheric corrosion tests, Brit. Corros. J. 20 (1985) 117–124.
[15] NACE No. 2/SSPC-SP 10, White Metal Blast Cleaning, NACE International, 2013.
[16] ASTM D1141 – 98, Standard Practice for the Preparation of Substitute Ocean Water, ASTM International, 2013.
[17] DNV-RP-B401, Cathodic Protection Design, Det Norske Veritas, 2010.
[18] P. Schmuki, S. Virtanen, H.S. Isaacs, Cathodic reduction of passive films on iron in borate and Phosphate buffer ph 8.4: different mechanisms revealed by in situ techniques, in: Proceedings of the 199th Meeting of the Electrochemical Society, 2001, pp. 178–186.
[19] R.A. Oriani, Hydrogen embrittlement of steels, Annu. Rev. Mater. Sci. 8 (1978) 327–357.

[20] D. Hardie, E.A. Charles, A.H. Lopez, Hydrogen embrittlement of high strength pipeline steels, Corros. Sci. 48 (2006) 4378–4385.
[21] EN 12954, Cathodic protection of buried or immersed metallic structures, General principles and application for pipelines, European Standard, 2014.
[22] E. Miranda, M. Bethencourt, F.J. Botana, M.J. Cano, J.M. Sánchez-Amaya, A. Corzo, J. Garcíade Lomas, M.L. Fardeau, B. Olliviera, Biocorrosion of carbon steel alloys by an hydrogenotrophic sulfate-reducing bacterium Desulfovibrio capillatus isolated from a Mexican oil field separator, Corros. Sci. 48 (2006) 2417–2431.
[23] Sahar A. Fadl-allah, A.A. Montaser, Sanaa M.F. Gad, El-Rab, Biocorrosion control of electroless Ni-Zn-P coating based on carbon steel by the pseudomonas aeruginosa biofilm, Int. J. Electrochem. Soc. 11 (2016) 5490–5506.